



Drag Polar Invariance with Flexibility

Jean-Luc Hantrais-Gervois, Daniel Destarac

► To cite this version:

Jean-Luc Hantrais-Gervois, Daniel Destarac. Drag Polar Invariance with Flexibility. Journal of Aircraft, 2015, 52 (3), pp.1-5. <10.2514/1.C033193>. <hal-01225671>

HAL Id: hal-01225671

<https://hal.science/hal-01225671v1>

Submitted on 13 Apr 2022

HAL is a multi-disciplinary open access archive for the deposit and dissemination of scientific research documents, whether they are published or not. The documents may come from teaching and research institutions in France or abroad, or from public or private research centers.

L'archive ouverte pluridisciplinaire **HAL**, est destinée au dépôt et à la diffusion de documents scientifiques de niveau recherche, publiés ou non, émanant des établissements d'enseignement et de recherche français ou étrangers, des laboratoires publics ou privés.



Distributed under a Creative Commons CC BY-NC 4.0 - Attribution - Non-commercial use - International License

Drag Polar Invariance with Flexibility

J.-L. Hantrais-Gervois* and D. Destarac†

ONERA–The French Aerospace Lab, 92190 Meudon, France

I. Introduction

MOST modern transport aircraft wings exhibit high aspect ratios (typically nine), and consequently undergo large deformations between ground and cruise, and beyond. The most noticeable effect is bending. A large bending modification will strongly contribute to the twist law alteration, and twist is a major aerodynamic parameter. Wind-tunnel models undergo smaller deformations than flying aircraft, but these are often by no means negligible. Their aerodynamic effects can be quantified in pressurized wind tunnels by changing dynamic pressure. They can also be modeled by aeroelastic computational simulations.

A puzzling thing is that, often in wind-tunnel tests, the effect is obvious on $C_L(\alpha)$, $C_m(\alpha)$, and $C_L(C_m)$ curves but almost indiscernible on $C_L(C_D)$ drag polars. The same phenomenon can happen with numerical simulations comparing a rigid-wing polar and a flexible-wing polar.

It is the purpose of this Note to explain under which conditions this phenomenon may take place.

II. Aeroelasticity

A. Aeroelastic Deformations of an Aircraft Wing

Aeroelastic effects are the coupled effects between the two disciplines: aerodynamics and mechanics. We set aside here unsteady interactions (flutter, buffeting) and consider the following causes and effects:

1) The steady aerodynamic loading of the wing is sustained by the wing structure attached to the fuselage.

2) The deformations undergone by the structure change the wing shape, and thus the aerodynamics forces and moments.

From a structural point of view, usual civil aircraft wings can be considered as cantilever beams with high aspect ratios. The main deformation undergone by the wing is bending. Bending does not significantly affect the aerodynamics in a direct way; but due to the wing sweep, the aerodynamic profiles are twisted when the wing is bent. The bending-induced twist has a significant aerodynamic impact. The explanation (see, for instance, [1]) is illustrated by Fig. 1. Aerodynamic profiles lie in longitudinal planes ($y = cte$), whereas the bending deformation follows the beam direction, which is approximately the wing sweep. Therefore, identical Δz will be produced at the ends of the rib but different Δz at the ends of the aerodynamic profile, producing aerodynamic twist. In addition to bending, structural torsion due to moment also contributes to the aerodynamic twist; but in cruise conditions, this contribution is of a lower order.

At cruise, due to the aircraft weight evolution due to fuel burn and adjustments in altitude, the twist is not constant.

B. Flexibility in Experimental Fluid Dynamics

To understand why drag polars can be nearly invariant with flexibility, it is necessary to consider independently flexibility in experimental fluid dynamics (EFD) and in computational fluid dynamics (CFD).

In EFD, aeroelastic effects can appear as different wing shapes at the same nondimensional lift coefficient but for different absolute loads (in newtons) produced by different dynamic pressures. In flight, during cruise, the twist changes by about 1 deg at the tip (see [2]). Aircraft models are usually stiffer than real aircraft, but similar deformations can be achieved in pressurized wind tunnels, where dynamic pressure is a parameter.

On the $C_L(\alpha)$ curve, an increase in dynamic pressure induces an increase in the angle of attack to reach a given lift coefficient. As long as aerodynamics is linear, deformations (wing twist) are proportional to the load and the difference in angle of attack increases linearly with lift (decrease of the lift slope), as illustrated in Fig. 2.

But, the unloaded wing (around zero lift) will have a unique shape; see Fig. 2. Thus, the $C_L(\alpha)$ curve appears to rotate around the zero lift point.

C. Flexibility in Computational Fluid Dynamics

In CFD, aeroelastic effects appear in a different way. Wing stiffness is then a parameter. A rigid-wing computation simulates a wing with infinite stiffness. It is the limit case where the wing does not deform with lift. Between the rigid and the flexible shapes, the twist difference increases linearly with lift and the aerodynamic effect appears again as a rotation of the $C_L(\alpha)$ curve. But, there is an important difference with the situation in the wind tunnel.

In the wind tunnel, the basic shape is necessarily the zero load shape (the “jig shape”) that will deform under load, conforming to the “cruise shape” (or 1g shape) at cruise. In CFD, the basic shape is usually the cruise shape because it corresponds to the design shape. Thus, rigid-wing polars are computed with the cruise shape instead of the jig shape, which has no aerodynamic interest. So, the important difference with the wind-tunnel situation is that the $C_L(\alpha)$ curve now rotates around the cruise point instead of around the zero lift point (see Fig. 3). This is the key point to explain when and why drag polars may, or may not, be invariant with flexibility.

III. Numerical Investigation

A. Test Case and Numerical Tools

The test case considered here to investigate these effects is the HiReTT [3] wing–fuselage model. Representative of a large transport aircraft cruising at $M = 0.85$, it has been widely used in European projects. Reynolds-averaged Navier–Stokes simulations are carried out with the elsA software [4] with a finite volume discretization in structured grids. Far-field drag postprocessing yields physical drag component breakdown [5]. Drag is thus decomposed as lift-induced drag C_{Di} , viscous pressure drag C_{Dvp} , friction drag C_{Df} (obtained by surface integration instead of the far field analysis), and wave drag C_{Dw} .

Simulations are carried out with either a rigid flight shape or with adapted wing shapes to each lift coefficient, to simulate various wing flexibilities.

*Research Engineer, Applied Aerodynamics Department; Jean-Luc.Hantrais-Gervois@onera.fr.

†Research Engineer, Applied Aerodynamics Department; Daniel.Destarac@onera.fr.

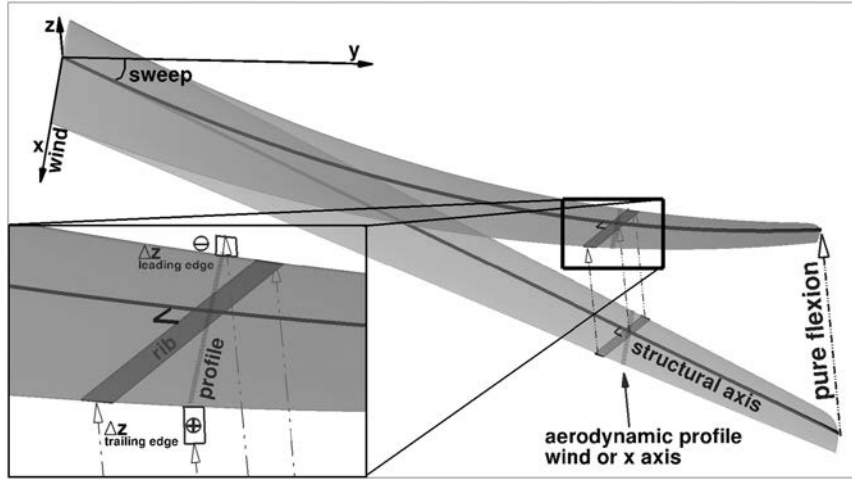


Fig. 1 Bending effect on the aerodynamic twist.

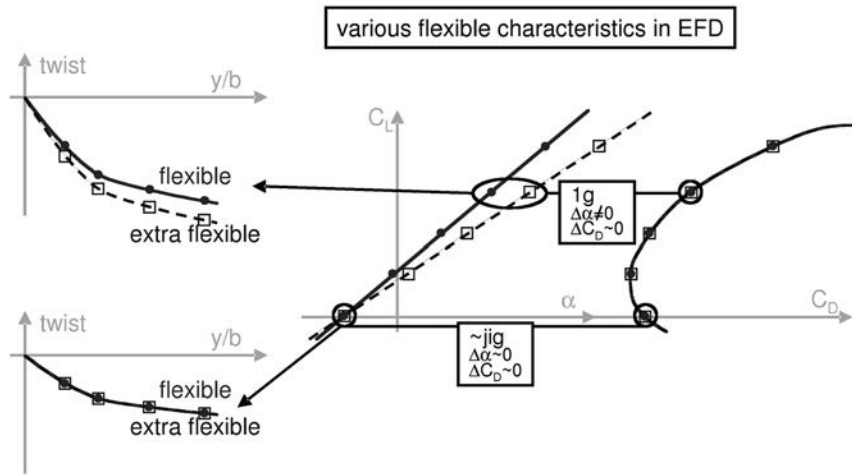


Fig. 2 Experimental flexibility effect.

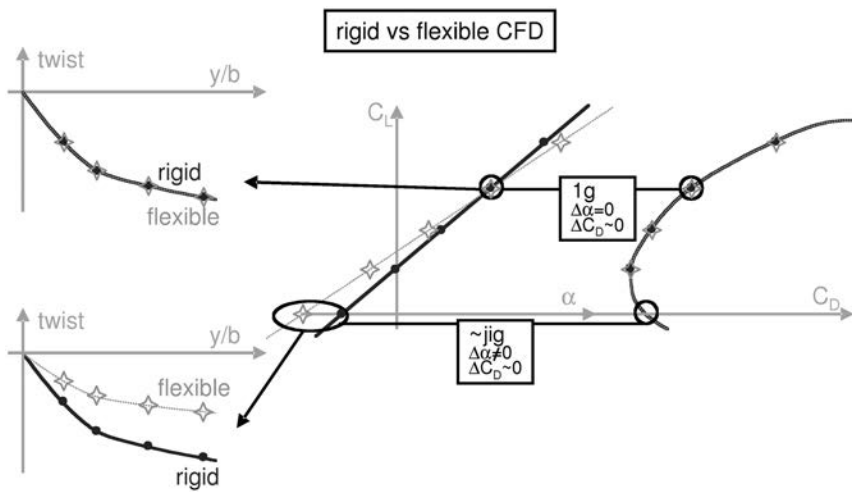


Fig. 3 Numerical flexibility effect.

B. Analysis

It has been explained in the previous section that there are two main points of interest over the lift polar as regards the phenomenon investigated here: zero lift conditions and cruise conditions. The lift polar rotates around the former in the experiment and around the latter in computations. Besides, they bound the part of the drag polar where the invariance may occur.

1. Analysis at Cruise

The cruise point is a design point. A drag sensitivity study to the wing twist around the design shape is carried out at a given C_L , with the simple parametric twist modifications illustrated in Fig. 4. Tip twist variations are in the range ± 2.5 deg around the design shape.

Far-field drag component variations with tip twist at fixed C_L are plotted in Fig. 5. It can be seen that the design shape is

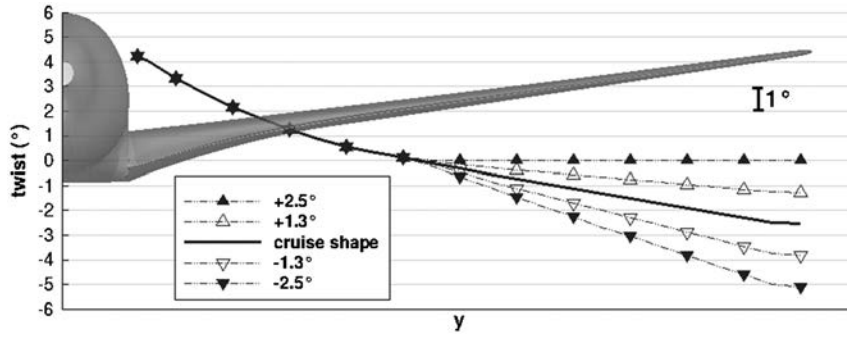


Fig. 4 Twist sensitivity studies at cruise.

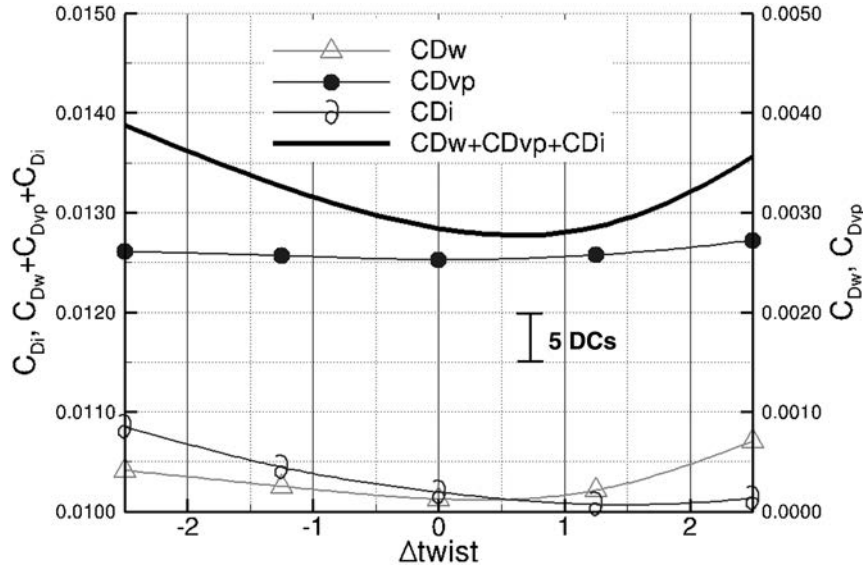


Fig. 5 Drag component evolutions with tip twist at cruise condition.

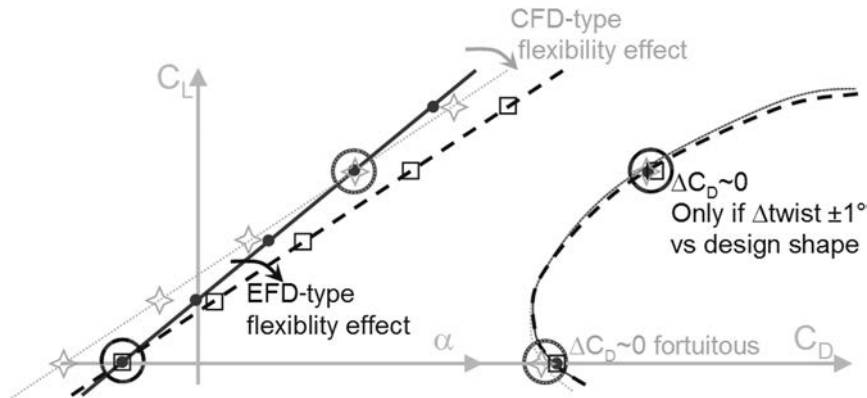


Fig. 6 Scheme of the experimental and numerical flexibility effects.

close to a drag optimum. Thus, in a range of about ± 1.3 deg at the tip, the drag is affected by less than four drag counts. In the range of ± 1 deg around the minimum drag, drag remains in a two-drag count band (see Fig. 6). In a wind-tunnel test, total pressure variations are unlikely to induce such a range of twist modification.

With respect to wave drag, the design shape is an optimum. Lift-induced drag could be improved with more noseup twist. This may reflect structural considerations in the design. Viscous pressure drag is marginally affected by twist.

2. Analysis at Zero Lift

It is not usual to perform drag analysis around zero lift because this point is of no interest for flight operations. Nevertheless, this point

corresponds to the center of rotation of the lift curve due to aeroelastic effects in experiments.

Besides the rigid cruise shape, two other shapes have been simulated. They correspond to zero lift shapes that would be achieved for more or less flexible wings and cover a range of 3.6 deg in noseup tip twist (see Fig. 7).

At this low angle of attack, the main aerodynamic features (shock patterns) are located on the pressure side and significant wave and viscous pressure drag is generated on the pressure side. Over the twist range, the differences in drag due to these components are limited to two drag counts.

Nevertheless, the drag analysis (see Fig. 8) reveals that an additional two-drag count difference is due to the lift-induced drag, for which absolute value is lower than five drag counts at zero lift.

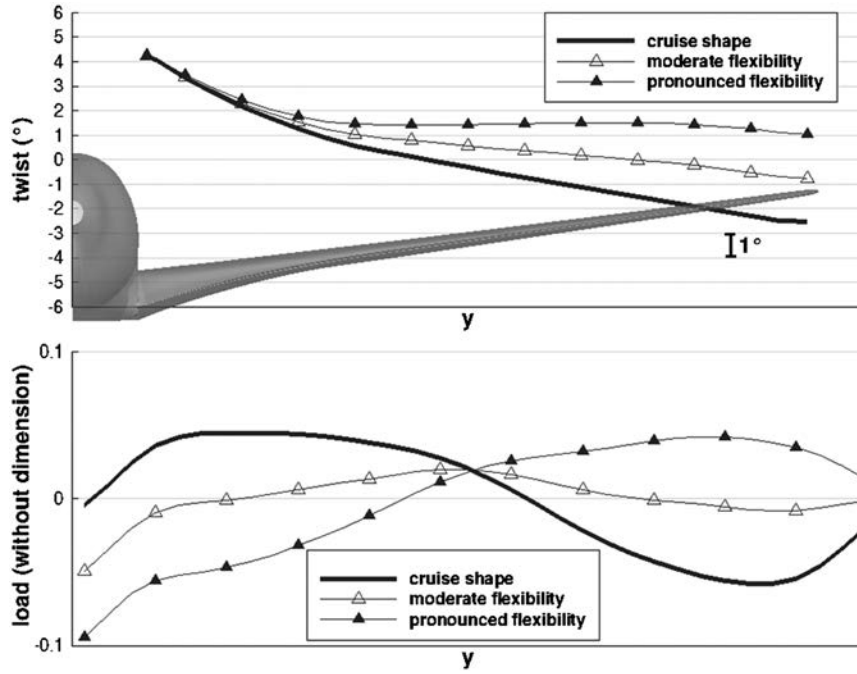


Fig. 7 Twist sensitivity studies at zero lift and span loading.

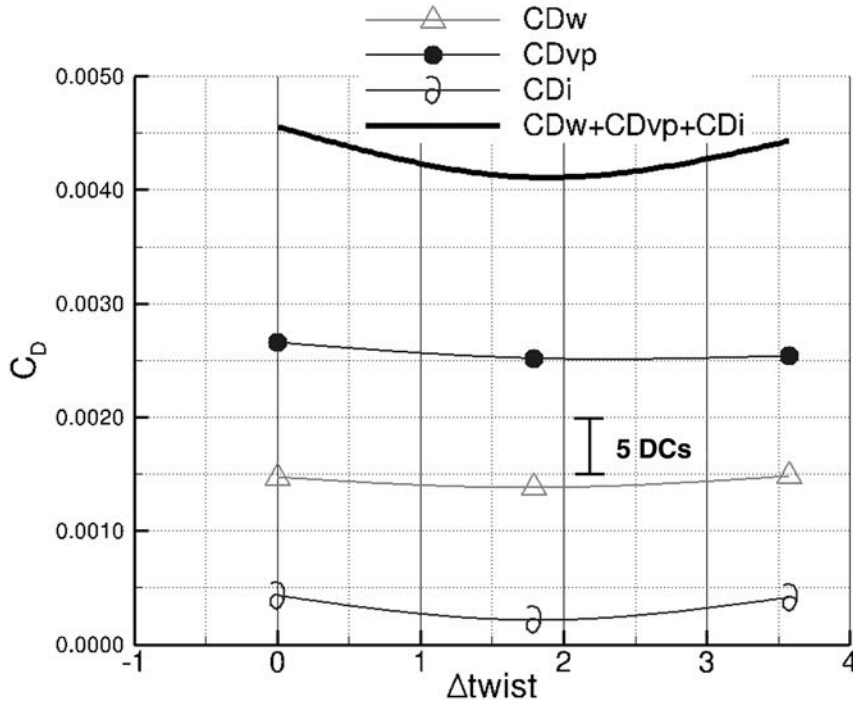


Fig. 8 Drag component evolutions with tip twist at zero lift condition.

Indeed, the spanwise lift distributions (see Fig. 7) exhibit significant differences as a result of different flows. The induced drag depending on the local lift times its derivative over the span; its value is the lowest for the moderate flexibility that exhibits a flat shape. On the contrary, the S-shaped lift distributions exhibited by the most distant twist laws (cruise shape and pronounced flexibility) correspond to higher lift-induced drag values. In that example, these curves correspond to significantly different flows but the curves are symmetrical according to the origin; thus, the induced drag values are identical.

A drag polar invariance is thus fortuitous and strongly depends on the configuration (see Fig. 6).

IV. Conclusions

The purpose of this Note is to establish the conditions of appearance of drag polar invariance through a flexibility effect.

Attention has been paid to the idiosyncrasies of flexibility effects in experiments on the one hand and in numerical simulations on the other hand. If both numerical and experimental effects are evidenced through a rotation of the $C_L(\alpha)$ curve, the center of rotation is not the same; thus, the conditions of appearance of drag polar invariance differ.

A detailed drag analysis has been carried out at the two key polar points for drag polar invariance: zero lift and cruise lift.

As for the experimental flexibility effect, the $C_L(\alpha)$ curve rotates around the zero lift point and the drag polar invariance depends on the aerodynamic behavior at the cruise point. This point being at or near a flat drag minimum through exchange between lift-induced drag, wave drag, and viscous pressure drag, the drag polar will be invariant around both points. It will remain so between the two points if wing twist variation is moderate. In the case analyzed here, invariance in the limit of two drag counts is obtained for a twist variation of ± 1 deg. Twist variations are usually under this limit in wind-tunnel tests and close to it in flight.

As for the numerical flexibility effect, the $C_L(\alpha)$ curve rotates around the cruise point and the drag polar invariance depends on the aerodynamic behavior at the zero lift point. Thus, in the case of numerical simulations, drag polar invariance at zero lift is fortuitous.

References

- [1] Wiert, L., and Carrier, G., "Accounting for Wing Flexibility in the Aerodynamic Calculation of Transport Aircraft Using Equivalent Beam Model," *13th AIAA/ISSMO Multidisciplinary Analysis Optimization Conference*, AIAA Paper 2010-9135, Sept. 2010.
- [2] Hantrais-Gervois, J.-L., and Rapin, M., "Aerodynamic and Structural Behaviour of a Wing Equipped with a Winglet at Cruise," *AIAA Aerospace Sciences Meeting and Exhibit*, AIAA Paper 2006-1489, Jan. 2006.
- [3] Rolston, S., and Elsholz, E., "Initial Achievements of the European High Reynolds Number Aerodynamic Research Project HiReTT," *40th AIAA Aerospace Science Meeting and Exhibit*, AIAA Paper 2002-0421, Jan. 2002.
- [4] Cambier, L., Heib, S., and Plot, S., "The Onera elsA CFD Software: Input from Research and Feedback from Industry," *Mechanics and Industry*, Vol. 14, No. 3, April 2013, pp. 159–174.
doi:10.1051/meca/2013056
- [5] van der Vooren, J., and Destarac, D., "Drag/Thrust Analysis of Jet-Propelled Transonic Transport Aircraft: Definition of Physical Drag Components," *Aerospace Science and Technology*, Vol. 8, No. 6, Sept. 2004, pp. 545–556.
doi:10.1016/j.ast.2004.03.004